ESC European Society of Cardiology

European Heart Journal (2022) **43**, 518–533
https://doi.org/10.1093/eurheartj/ehab644

TRANSLATIONAL RESEARCH
Vascular biology and medicine

Propionate attenuates atherosclerosis by immune-dependent regulation of intestinal cholesterol metabolism

Arash Haghikia [1,2,3]*, Friederike Zimmermann [1,2], Paul Schumann [1,2], Andrzej Jasina[1], Johann Roessler[1,2], David Schmidt [1], Philipp Heinze[1], Johannes Kaisler [4], Vanasa Nageswaran[1], Annette Aigner [3,5], Uta Ceglarek [6,7], Roodline Cineus [8,9], Ahmed N. Hegazy [3,8,9], Emiel P.C. van der Vorst [10,11,12,13], Yvonne Döring[10,11,14], Christopher M. Strauch [15], Ina Nemet [15], Valentina Tremaroli[16], Chinmay Dwibedi[16,17], Nicolle Kränkel [1,2], David M. Leistner [1,2,3], Markus M. Heimesaat [18], Stefan Bereswill[18], Geraldine Rauch[3,5], Ute Seeland[2,19], Oliver Soehnlein[10,11,20], Dominik N. Müller[2,3,21,22], Ralf Gold[4], Fredrik Bäckhed [16,23,24], Stanley L. Hazen [15,25], Aiden Haghikia[26†], and Ulf Landmesser [1,2,3†]

[1]Department of Cardiology, Charité—Universitätsmedizin Berlin, Campus Benjamin Franklin, Hindenburgdamm 30, 12203 Berlin, Germany; [2]German Center for Cardiovascular Research (DZHK), Partner Site Berlin, Berlin, Germany; [3]Berlin Institute of Health (BIH), Anna-Louisa-Karsch-Straße 2, Berlin 10178, Germany; [4]Department of Neurology, St. Josef-Hospital, Ruhr-University Bochum, Bochum, Germany; [5]Institute of Biometry and Clinical Epidemiology, Charité—Universitätsmedizin Berlin, Berlin, Germany; [6]Institute of Laboratory Medicine, Clinical Chemistry and Molecular Diagnostics, University Hospital Leipzig, Paul-List-Str. 13-15, Leipzig 04103, Germany; [7]LIFE-Leipzig Research Center for Civilization Diseases, University of Leipzig, Leipzig, Germany; [8]Department of Gastroenterology, Infectiology, and Rheumatology, Charité-Universitätsmedizin Berlin, Campus Benjamin Franklin, Hindenburgdamm 30, 12203 Berlin, Germany; [9]Deutsches Rheumaforschungszentrum Berlin (DRFZ), An Institute of the Leibniz Association, Berlin, Germany; [10]Institute for Cardiovascular Prevention (IPEK), LMU München, Munich, Germany; [11]German Center for Cardiovascular Research (DZHK), Partner Site Munich, Heart Alliance Munich, Munich, Germany; [12]Interdisciplinary Center for Clinical Research (IZKF), Institute for Molecular Cardiovascular Research (IMCAR), RWTH Aachen University, Pauwelsstraße 30, Aachen 52074, Germany; [13]Department of Pathology, Cardiovascular Research Institute Maastricht (CARIM), Maastricht University, Universiteitssingel 50, Maastricht 6200 MD, the Netherlands; [14]Departement of Angiology, Swiss Cardiovascular Center, Inselspital, Bern University Hospital, University of Bern, Murtenstrasse 35, Bern CH-3008, Switzerland; [15]Department of Cardiovascular & Metabolic Sciences, Lerner Research Institute, Cleveland Clinic, Cleveland, OH 44106, USA; [16]The Wallenberg Laboratory, Department of Molecular and Clinical Medicine, Institute of Medicine, Sahlgrenska Academy, University of Gothenburg, Bruna Stråket 16, Gothenburg SE-413 45, Sweden; [17]Institute of Neuroscience and Physiology, University of Gothenburg, Box 430, Gothenburg 405 30, Sweden; [18]Insitute of Microbiology, Infectious Diseases and Immunology, Charité—Universitätsmedizin Berlin, Hindenburgdamm 30, Berlin 12203, Germany; [19]Charité—Universitätsmedizin Berlin, Freie Universität Berlin, Humboldt-Universität zu Berlin, and Berlin Institute of Health, Institute of Social Medicine, Epidemiology and Health Economics, Campus Charité Mitte Luisenstraße 57, Berlin 10117, Germany; [20]Institute for Experimental Pathology (ExPat), Center for Molecular Biology of Inflammation (ZMBE), Von-Esmarch-Straße 56, WWU Münster 48149, Germany; [21]Experimental and Clinical Research Center, a joint cooperation of Max Delbrück Center for Molecular Medicine and Charité-Universitätsmedizin Berlin, Berlin, Germany; [22]Max Delbrück Center for Molecular Medicine in the Helmholtz Association, Robert-Rössle-Str. 10, Berlin 13092, Germany; [23]Novo Nordisk Foundation Center for Basic Metabolic Research, Faculty of Health and Medical Sciences, University of Copenhagen, Blegdamsvej 3B, Copenhagen DK-2200, Denmark; [24]Department of Clinical Physiology, Region Västra Götaland, Sahlgrenska University Hospital, Box 430, Gothenburg 405 30, Sweden; [25]Department of Cardiovascular Medicine, Heart and Vascular Institute, Cleveland Clinic, 9500 Euclid Ave., NC-10 Cleveland 44195, OH, USA; and [26]Department of Neurology, Otto-von-Guericke University, Leipziger Str. 44, Magdeburg 39120, Germany

Received 29 January 2021; revised 30 June 2021; editorial decision 26 August 2021; accepted 1 September 2021; online publish-ahead-of-print 1 October 2021

See the editorial comment for this article 'The promise of the gut metabolite propionate for a novel and personalized lipid-lowering treatment', by Elena Osto, https://doi.org/10.1093/eurheartj/ehab723.

Aims Atherosclerotic cardiovascular disease (ACVD) is a major cause of mortality and morbidity worldwide, and increased low-density lipoproteins (LDLs) play a critical role in development and progression of atherosclerosis. Here, we examined for the first time gut immunomodulatory effects of the microbiota-derived metabolite propionic acid (PA) on intestinal cholesterol metabolism.

Methods and results Using both human and animal model studies, we demonstrate that treatment with PA reduces blood total and LDL cholesterol levels. In apolipoprotein $E^{-/-}$ (*Apoe*$^{-/-}$) mice fed a high-fat diet (HFD), PA reduced intestinal cholesterol

* Corresponding author. Tel: +49 30 450 513 638, Fax: +49 30 450 513 996, Email: arash.haghikia@charite.de
† These authors contributed equally as senior authors.

absorption and aortic atherosclerotic lesion area. Further, PA increased regulatory T-cell numbers and interleukin (IL)-10 levels in the intestinal microenvironment, which in turn suppressed the expression of Niemann-Pick C1-like 1 (Npc1l1), a major intestinal cholesterol transporter. Blockade of IL-10 receptor signalling attenuated the PA-related reduction in total and LDL cholesterol and augmented atherosclerotic lesion severity in the HFD-fed *Apoe*$^{-/-}$ mice. To translate these preclinical findings to humans, we conducted a randomized, double-blinded, placebo-controlled human study (clinical trial no. NCT03590496). Oral supplementation with 500 mg of PA twice daily over the course of 8 weeks significantly reduced LDL [-15.9 mg/dL (-8.1%) vs. -1.6 mg/dL (-0.5%), $P = 0.016$], total [-19.6 mg/dL (-7.3%) vs. -5.3 mg/dL (-1.7%), $P = 0.014$] and non-high-density lipoprotein cholesterol levels [PA vs. placebo: -18.9 mg/dL (-9.1%) vs. -0.6 mg/dL (-0.5%), $P = 0.002$] in subjects with elevated baseline LDL cholesterol levels.

Conclusion Our findings reveal a novel immune-mediated pathway linking the gut microbiota-derived metabolite PA with intestinal Npc1l1 expression and cholesterol homeostasis. The results highlight the gut immune system as a potential therapeutic target to control dyslipidaemia that may introduce a new avenue for prevention of ACVDs.

Graphical Abstract

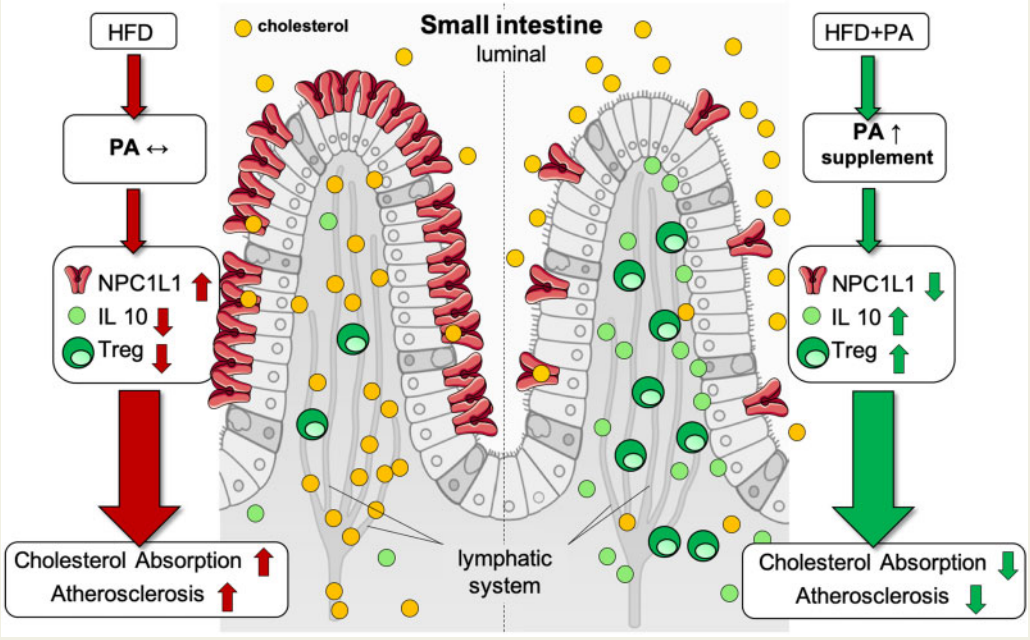

The figure illustrates the proposed model of the cholesterol-lowering and atheroprotective properties of propionate. A high-fat high-cholesterol diet causes a disbalance of immune cells in the small intestinal microenvironment, with reduced regulatory T cell frequencies and interleukin-10 concentrations. Altered regulatory T cell levels are rescued upon exogenous propionate supplementation, with increased local levels. This in turn modulates NPC1L1 expression and membrane density, with a subsequent reduction in cholesterol absorption, ultimately leading to reduced atherogenesis. The illustration was adopted from Servier Medical Art (http://smart.servier.com/), licensed under a Creative Common Attribution 3.0 Generic License. HFD, high-fat diet; IL-10, interleukin-10; NPC1L1, Niemann-Pick C1-like 1; PA, propionic acid; Treg, regulatory T cell.

Keywords Gut microbiome • Propionic acid • Atherosclerosis

Translational perspective

Our study identifies a novel regulatory circuit that links the gut microbiota metabolite propionic acid (PA), a short-chain fatty acid, with the gut immune system to control intestinal cholesterol homeostasis and prevent the development of atherosclerosis. This mechanism involves PA-mediated increase in regulatory T-cell numbers and interleukin-10 levels in the intestinal microenvironment, which in turn suppresses the expression of Niemann-Pick C1-like 1, a major intestinal cholesterol transporter. In a proof-of-concept clinical study, we demonstrate that oral supplementation of PA over the course of 8 weeks significantly reduced low-density lipoprotein and non-high-density lipoprotein cholesterol levels in subjects with hypercholesterolaemia.

Our findings suggest that supplementation of PA may improve cholesterol homeostasis and contribute to cardiovascular health. Another translational outlook is the modulation of the gut microbiome, e.g. by dietary approaches or by prebiotics to sustainably increase the intestinal abundance of PA producing bacteria as a novel intrinsic concept of atheroprotection.

Introduction

Atherosclerotic cardiovascular diseases (ACVDs) are a major global health care burden and a leading cause of mortality and morbidity worldwide.[1] Elevated levels of low-density lipoprotein (LDL) and non-high-density lipoprotein (non-HDL) cholesterol are important modifiable risk factors for ACVD, thus representing a major effective target for ACVD prevention.[2,3] In recent years, increasing attention has been devoted to identifying gut microbial pathways affecting metabolic pathways[4] or atherogenesis.[5–7] In particular, gut microbiota-derived metabolites that are transported to the peripheral circulation in the host via the portal vein can act as signalling molecules and may impact atherogenesis by regulating host metabolism,[8] immune homeostasis,[9] and vascular function.[10,11]

Among detrimental metabolites, trimethylamine N-oxide, generated by gut microbial metabolism of trimethylamine-containing nutrients such as choline and carnitine, has been shown to promote the development of atherosclerosis in animal models[5,6,12] with prognostic implications for patients with coronary heart disease,[13] chronic kidney disease,[14] ischaemic stroke,[15] and mortality.[16] Short-chain fatty acids (SCFAs; i.e. acetic, propionic, and butyric acids) derived by gut microbial fermentation of dietary fibres, on the other hand, have shown beneficial effects on host metabolism and cardiac health.[17,18] Although SCFAs are primarily considered important energy sources in intestinal epithelial cells, they also possess regulatory properties and affect host metabolism, immune homeostasis, and cell proliferation.[17] Propionic acid (PA) has been shown to critically regulate T-cell-mediated immunity and thereby modulate the disease course in autoimmune diseases, particularly by promoting the differentiation and functional capacity of CD25+ Foxp3+ regulatory T cells (Tregs).[19–21] PA also has been reported to promote beneficial effects on cardiac remodelling in experimental hypertension by counteracting hypertension-induced imbalance between Tregs and effector T cells.[22] Epidemiological studies suggest that sufficient fibre intake may contribute to preventing dyslipidaemia and atherosclerotic vascular disease.[23] However, the underlying mechanisms remain unclear. Tregs have been reported to have the ability to modulate cholesterol metabolism and subsequent atheroprotective effects,[24] which raises the question of whether SCFAs may regulate lipids in an immune-dependent way.

Here, we examine for the first time pathways whereby the microbiome-derived SCFA PA may regulate lipoprotein levels that are causal for atherosclerotic lesion development in hypercholesterolaemic and atherosclerosis-prone apolipoprotein E (*Apoe*)$^{-/-}$ mice. Moreover, in a proof-of-concept double-blind and placebo-controlled clinical study, the effect of PA on LDL and total cholesterol levels was evaluated in humans with hypercholesterolaemia.

Results

Short-chain fatty acid propionate prevents high-fat diet-induced hypercholesterolaemia and atherosclerosis in *Apoe*$^{-/-}$ mice

We first evaluated gut microbiota-dependent control of plasma lipids using conventionally raised and antibiotic treated *Apoe*$^{-/-}$ mice (ABS) with a depleted gut microbiota that were fed either a standard chow (SCD) or high-fat diet (HFD) for 6 weeks. In mice with a depleted gut microbiota, we found increased levels of total, very low-density lipoprotein (VLDL), and LDL cholesterol compared to those of conventionally raised *Apoe*$^{-/-}$ mice under an SCD and an HFD (*Figure 1A–F*). These findings support a functional role of gut microbiota-dependent metabolic pathways in the control of blood cholesterol levels. The increase in cholesterol levels was accompanied by increased atherosclerotic lesion size after 6 weeks of either diet (*Figure 1G and H*). Next, we examined the effect of exogenous PA administered via daily oral gavage on plasma lipids in hypercholesterolaemic *Apoe*$^{-/-}$ mice (*Figure 2A*). We observed that treatment with PA (200 mg/kg) prevented HFD-induced increases in total, VLDL, and LDL cholesterol (*Figure 2B and F*).

Importantly, the vehicle used for oral gavage (0.9% sodium chloride) did not have any relevant effects on blood lipids metabolism (Supplementary material online, *Figure S1*). Moreover, HFD increased several cholesteryl esters, some of which were reduced upon treatment with PA (Supplementary material online, *Figure S2*). Consequently, the HFD-induced increase in atherosclerotic lesion size was attenuated by PA (*Figure 2G and H*).

Notably, PA treatment significantly lowered total, LDL and VLDL cholesterol in antibiotic treated and HFD-fed *Apoe*$^{-/-}$ mice (Supplementary material online, *Figure S3A–E*) demonstrating that PA can compensate for the de-regulated intestinal cholesterol metabolism in gut microbiota-depleted mice. Treatment with PA also tended to attenuate atherosclerotic lesion size in antibiotic treated and HFD-fed *Apoe*$^{-/-}$ mice, although this effect did not reach statistical significance (Supplementary material online, *Figure S3F and G*) suggesting that gut microbial-dependent anti-atherogenic mechanisms go beyond intestinal cholesterol regulation.

Propionate impacts intestinal cholesterol metabolism by modulating the expression of Niemann-Pick C1-like protein 1

To further understand the mechanisms underlying PA-mediated lipid regulation, we determined the expression of major genes involved in hepatic cholesterol metabolism. We found up-regulated expression of sterol regulatory element-binding protein (*Srebp2*) and cholesterol 7 alpha-hydroxylase (*Cyp7a1*) in hypercholesterolaemic *Apoe*$^{-/-}$ mice, of which only the up-regulated expression of *Srebp2* was reversed upon PA treatment (*Figure 3A and B*). Other genes involved in hepatic cholesterol and bile acid synthesis, including LDL receptor (*Ldlr*) (*Figure 3C*), proprotein convertase subtilisin/kexin type 9 (*Pcsk9*), 3-hydroxy-3-methyl-glutaryl-coenzyme A (HMG-CoA) reductase (*Hmgcr*), and farnesoid X receptor (*Fxr*), were not significantly altered by HFD or additional PA treatment (Supplementary material online, *Figure S4A–C*). Next, we sought to investigate whether PA impacts the activity of HMG-CoA reductase, the rate-controlling enzyme of cholesterol synthesis. However, the enzymatic activity of HMG-CoA reductase was not affected by PA at increasing concentrations (Supplementary material online, *Figure S4D*). These findings argue against a relevant role of PA in hepatic regulation of cholesterol metabolism. Beside Hepatic cholesterol clearance and synthesis, intestinal cholesterol metabolism, particularly cholesterol trafficking and

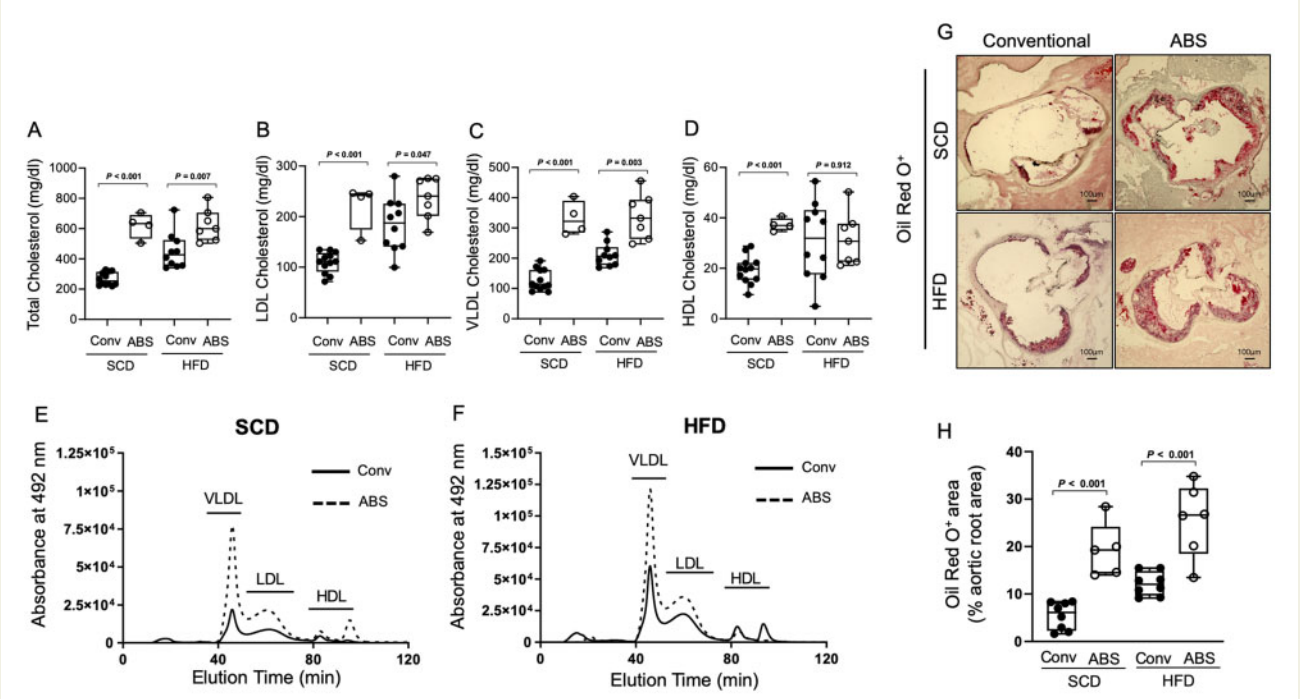

Figure 1 The gut microbiota regulates cholesterol metabolism and impacts atherogenesis. (*A–D*) HPLC analysis of blood levels of total cholesterol, low-density lipoprotein cholesterol, very low-density lipoprotein cholesterol and high-density lipoprotein cholesterol in conventionally raised (Conv, black circles) or antibiotic treated (ABS, white circles) *Apoe*$^{-/-}$ mice fed either a standard chow or a high-fat diet (Conv: standard chow $n = 12$, high-fat diet $n = 10$; ABS: standard chow $n = 4$, high-fat diet $n = 7$). (*E* and *F*) Representative HPLC-assisted fractionation of plasma lipids under a standard chow or a high-fat diet. (*G* and *H*) Representative images of Oil Red O-stained aortic root sections (scale bars represent 100 μm) with quantification of lipid deposition (Conv, black circles: standard chow $n = 8$, high-fat diet $n = 8$; ABS, white circles: standard chow $n = 5$, high-fat diet $n = 6$). Data were analysed by a two-tailed unpaired *t*-test between two groups. HDL, high-density lipoprotein; HFD, high-fat diet; HPLC, High-performance liquid chromatography; LDL, low-density lipoprotein; SFD, standard chow; VLDL, very low-density lipoprotein.

absorption, are key components of cholesterol homeostasis.[25] We therefore investigated a potential regulatory role of PA on intestinal expression of Niemann-Pick C1-like protein 1 (*Npc1l1*), a major transmembrane transporter responsible for intestinal cholesterol absorption.[26] We also examined the impact of PA on the expression of apical sodium–bile acid transporter (*Asbt*), which mediates active uptake of conjugated bile acids[27] to maintain their enterohepatic recirculation. While PA normalized the HFD-induced increase in *Npc1l1* gene expression in the small intestine, it did not affect HFD-induced *Asbt* expression (*Figure 3D and E*). Increased density of NPC1L1 was also observed in histological sections of the small intestine from *Apoe*$^{-/-}$ mice fed with HFD compared to mice fed with SCD and was prevented in HFD-fed mice under PA treatment (*Figure 3F and G*). Interestingly, we found no significant differences in the expression of genes regulating the flux of lipids across small intestinal enterocytes, including ATP-binding cassette subfamily G member 5 (*Abcg5*), acetyl-CoA acetyltransferase (*Acat2*), and ATP-binding cassette transporter 1 (*Abca1*), between PA-treated and -untreated mice (Supplementary material online, Figure S5A–C). Next, we investigated the functional relevance of altered *Npc1l1* expression and analysed plasma levels of the phytosterols stigmasterol and sitosterol in *Apoe*$^{-/-}$ mice that were fed with SCD or HFD with or without PA. Since the abundance of plasma phytosterol depends on dietary intake and intestinal sterol absorption capacity, plasma levels of phytosterols serve as an indicator of the intestinal sterol absorption rate.[28] We found increased levels of both stigmasterol and sitosterol in mice fed with HFD, and this change was prevented upon treatment with PA (*Figure 3H and I*). Moreover, we found increased levels of faecal cholesterol in HFD-fed mice treated with PA as compared to mice without PA treatment (Supplementary material online, *Figure S6*). These observations suggested that PA modulates intestinal sterol absorption capacity, which is in line with the observed down-regulation of *Npc1l1* by PA. We used a mouse intestinal epithelial organoid culture system after specific expansion of adult intestinal stem cells[29] to examine the regulatory role of PA in modulating *Npc1l1*. Interestingly, treatment of the intestinal organoids with different concentrations of PA revealed no significant effect of PA on the expression of the *Npc1l1* gene (Supplementary material online, *Figure S7*), suggesting a more complex regulation of *Npc1l1* by PA.

Treatment with propionate increases regulatory T cells and interleukin-10 in the small intestine

In view of recent insights into the modulatory effects of PA on intestinal T-cell immunity,[20,30] and growing evidence for the involvement

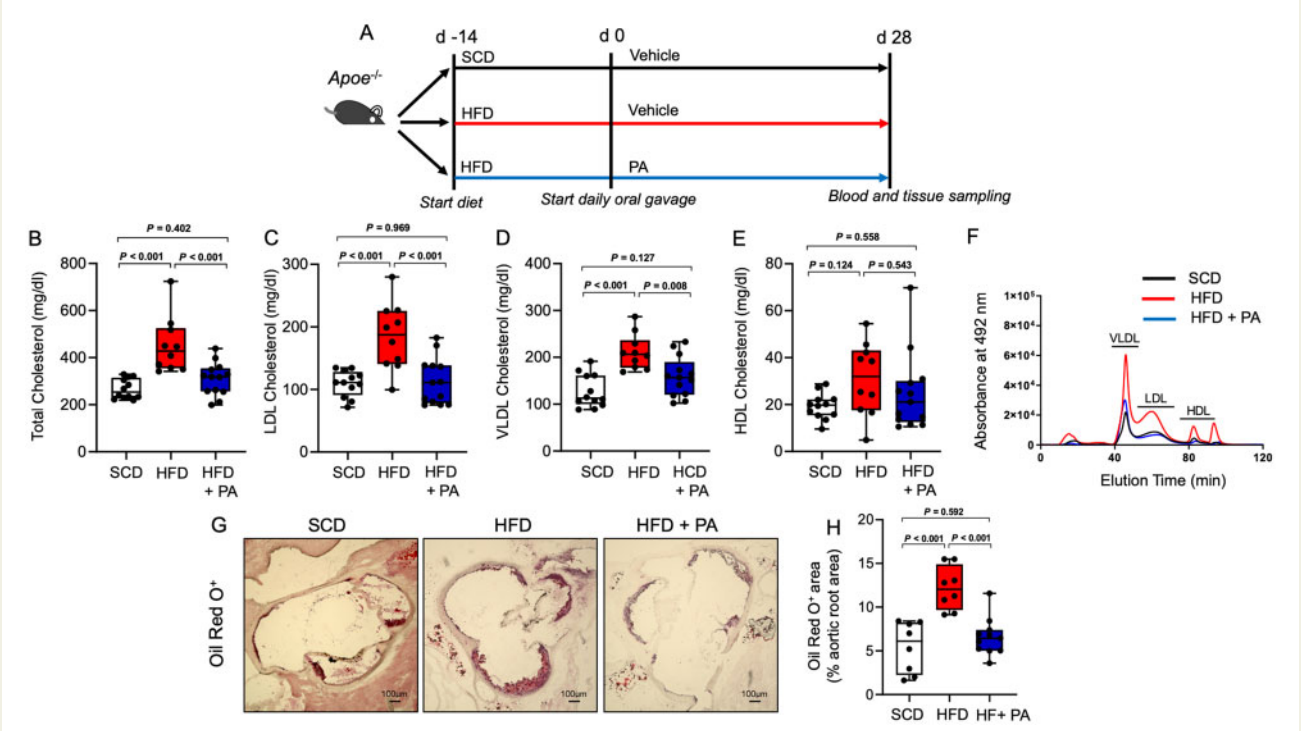

Figure 2 Propionate prevents high-fat diet-induced hypercholesterolaemia and atherosclerosis in *Apoe*$^{-/-}$ mice. (*A*) *Apoe*$^{-/-}$ mice were fed either a standard chow diet (standard chow, $n = 12$) or a high-fat diet (high-fat diet, $n = 24$) for 6 weeks. After 2 weeks, the standard chow-fed mice received sodium chloride (vehicle), and the high-fat diet-fed mice were treated with either propionate (propionic acid, $n = 13$) or sodium chloride (vehicle, $n = 11$) via oral gavage until the end of the experiment. (*B–E*) HPLC analysis of blood levels of total cholesterol, low-density lipoprotein cholesterol, very low-density lipoprotein cholesterol and high-density lipoprotein cholesterol in *Apoe*$^{-/-}$ mice at the end of the experiments (standard chow $n = 12$, high-fat diet $n = 10$, high-fat diet + propionic acid $n = 13$). (*F*) Representative HPLC-assisted fractionation of plasma lipids. (*G* and *H*) Representative images of Oil Red O-stained aortic root sections (scale bars represent 100 µm) with quantification of lipid deposition (standard chow $n = 8$, high-fat diet $n = 8$, high-fat diet + propionic acid $n = 11$). For the analysis in (*B–H*), the results of the Conv standard chow and Conv high-fat diet groups were the same results used in *Figure 1*. Data were analysed by one-way ANOVA followed by *post hoc* Tukey's test. HDL, high-density lipoprotein; HFD, high-fat diet; LDL, low-density lipoprotein; PA, propionic acid; SFD, standard chow; VLDL, very low-density lipoprotein.

of intestinal T cells in the control of systemic metabolism,[31] we hypothesized that modulation of the intestinal adaptive immune system at least partly mediates PA-related alterations in cholesterol metabolism. In line with previous reports[20,30] we observed an increase of CD25+ Foxp3+ Tregs in the mesenteric lymph nodes (MLNs) and the peripheral circulation (*Figure 4A–C*) of HFD-fed *Apoe*$^{-/-}$ mice in response to PA. Notably, the splenic Treg population was not altered, suggesting that the small intestine was the primary source of the increase in Tregs in response to PA in our model (*Figure 4D*). Notably, we did not observe alterations in T helper 1 (Th1) or Th17 cell frequencies in the MLNs, peripheral circulation or spleen upon PA treatment (Supplementary material online, *Figure S8A–F*). The increase in the Treg cell population in response to PA was accompanied by increased concentrations of interleukin (IL)-10, the major Treg cytokine, in the small intestinal wall (*Figure 4E*). Other cytokines related to Th1 or Th17 cells or monocytes, including tumour necrosis factor-alpha, monocyte chemoattractant protein-1, IL-6, and interferon gamma, were not altered by PA (*Figure 4F–I*).

Interleukin-10 regulates the intestinal expression of Niemann-Pick C1-like protein 1

To examine potential regulation of the *Npc1l1* gene by IL-10, we used mouse intestinal epithelial organoids (*Figure 5A*), which express both the IL-10R1 and IL-10R2 receptors[32] (*Figure 5B*). Treatment with recombinant mouse IL-10 induced dose-dependent down-regulation of *Npc1l1* gene expression (*Figure 5C*). To further explore the functional relevance of IL-10-dependent regulation of *Npc1l1* gene expression for PA-related intestinal cholesterol metabolism and atheroprotection, we blocked IL-10 signalling using an anti-IL-10 receptor monoclonal antibody (AB), which was intraperitoneally injected once per week during the PA treatment period (*Figure 5D*). Blockade of IL-10 receptor signalling attenuated the PA-related lowering effect on total, LDL, VLDL, and HDL cholesterol (*Figure 5E–I*) and augmented atherosclerotic lesion severity in HFD-fed *Apoe*$^{-/-}$ mice (*Figure 5J and K*). Notably, inhibition of IL-10 receptor signalling

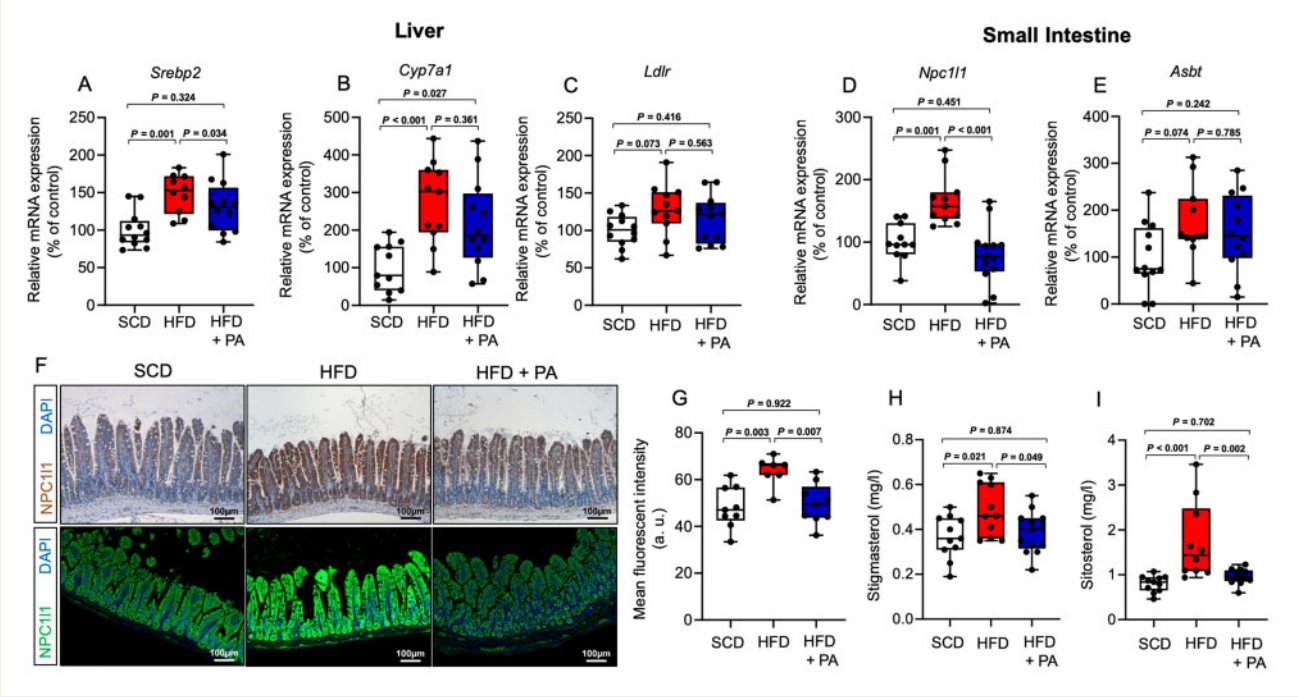

Figure 3 Effect of propionate on expression of genes involved in hepatic and intestinal cholesterol metabolism. (*A–E*) Expression of hepatic *Srebp2, Cyp7a1, Ldlr*, and small intestinal *Npc1l1* and *Asbt*, as assessed by quantitative polymerase chain reaction at the end of the treatment (standard chow $n = 11–12$, high-fat diet $n = 10–11$ and high-fat diet + propionic acid $n = 12–13$). (*F*) Representative immunostaining (scale bars represent 100 µm) of the small intestine of mice using an NPC1L1 antibody (upper row, immunohistochemistry; lower row, immunofluorescence) with (*G*) quantification of the mean fluorescence intensity (standard chow $n = 9$, high-fat diet $n = 7$ and high-fat diet + propionic acid $n = 9$). (*H* and *I*) Analysis of blood levels of the phytosterols stigmasterol and sitosterol at the end of the experiments (standard chow $n = 11$, high-fat diet $n = 10–11$, high-fat diet + propionic acid $n = 13$). Data were analysed by one-way ANOVA followed by *post hoc* Tukey's test. HFD, high-fat diet; PA, propionic acid; SFD, standard chow.

resulted in elevated phytosterol plasma levels (*Figure 5L and M*), which is indicative of enhanced intestinal sterol absorption.

These findings support a regulatory circuit in which PA-induced elevations of Treg cell frequency and local IL-10 concentrations in the small intestine regulate the expression of the major sterol transporter NPC1L1. Thereby, PA indirectly regulates the absorption of cholesterol, with subsequent implications for the development of hyperlipidaemia-induced atherosclerosis in *Apoe*$^{-/-}$ mice.

Propionic acid reduces serum low-density lipoprotein and total cholesterol in hypercholesterolaemic humans

To explore the clinical relevance of our findings, we performed a randomized, double-blind and placebo-controlled study in hypercholesterolaemic subjects evaluating the effect of oral supplementation of PA on LDL cholesterol blood levels as a primary endpoint and total, non-HDL and HDL cholesterol levels among the secondary endpoints (trial profile shown in Supplementary material online, *Figure S9*). A total of 62 individuals with baseline LDL cholesterol levels >115 mg/dL were enrolled and underwent 1:1 randomization to receive either oral placebo (500 mg) twice daily or PA (500 mg) twice daily for 8 weeks. The baseline clinical characteristics and biochemical parameters did not differ between the two study groups (*Table 1*). Study participants were advised to maintain their regular physical activity and dietary habits during the study period (dietary information shown in Supplementary material online, *Table S1*).

After 8 weeks, PA lowered LDL cholesterol levels [PA vs. placebo: -15.9 mg/dL (-8.1%) vs. -1.6 mg/dL (-0.5%), $P = 0.016$] and total cholesterol levels [PA vs. placebo -19.6 mg/dL (-7.3%) vs. -5.3 mg/dL (-1.7%), $P = 0.014$] compared to placebo (*Figure 6A–D*). Moreover, PA lowered non-HDL cholesterol levels [PA vs. placebo: -18.9 mg/dL (-9.1%) vs. -0.6 mg/dL (-0.5%), $P = 0.002$], whereas no significant difference in the change in HDL cholesterol levels [PA vs. placebo: -0.7 mg/dL (-0.9%) vs. -4.7 mg/dL (-6.0%), $P = 0.078$] was observed between the groups (*Figure 6E–H*). Notably, since the majority of study participant is represented by women (*Table 1*), in a subanalysis we evaluated the change in LDL and total cholesterol levels in male study participants and found a significant reduction in LDL {difference between: mean [95% confidence interval (CI)]: -15.75 (-31.31 to -0.18); $P = 0.048$} as well as in total cholesterol [difference between: mean (95% CI): -23.12 (-41.45 to -4.79); $P = 0.018$] upon PA supplementation as compared to placebo pointing to a sex-independent cholesterol-lowering effect of PA. No significant difference was observed for the change in body weight (*Figure 7A and B*). The safety and tolerability parameters were similar between the placebo and PA groups (*Table 2*), with no PA-related severe adverse

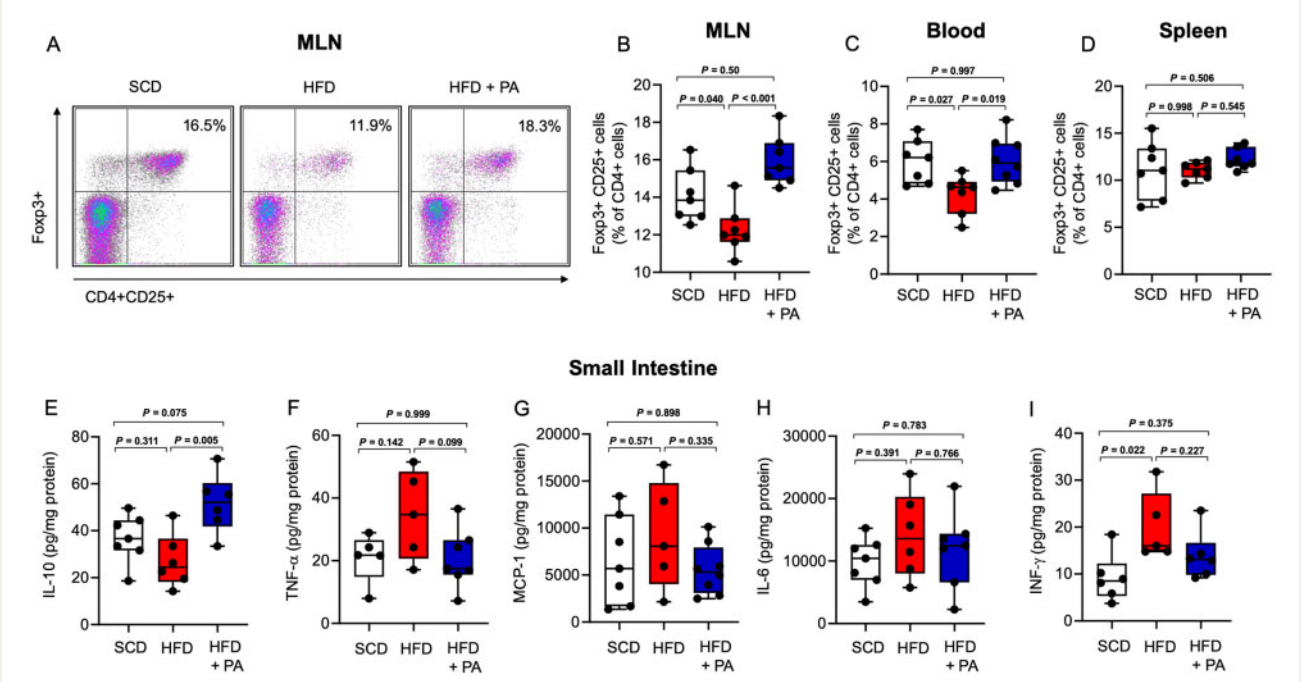

Figure 4 Treatment with propionate increases regulatory T cells and interleukin-10 in the small intestine. (*A*) Representative FACS plots of regulatory T cells in the mesenteric lymph nodes from mice in the standard chow, high-fat diet and high-fat diet + propionic acid groups. (*B* and *C*) Compared to the standard chow ($n = 7$), the high-fat diet ($n = 7$) reduced regulatory T cells in the mesenteric lymph nodes and peripheral blood, and this change was reversed by propionic acid treatment ($n = 7$–8). (*D*) Regulatory T cells in the spleen were not altered by high-fat diet or propionic acid. (*E*–*I*) Cytokine analysis of the small intestine revealed an increase in interleukin-10 levels after treatment with propionic acid, whereas the levels of tumour necrosis factor-alpha, monocyte chemoattractant protein-1, interleukin-6 and interferon gamma were not altered by propionic acid. Data were analysed by one-way ANOVA followed by *post hoc* Tukey's test. HFD, high-fat diet; IFN-γ, interferon gamma; IL-10, interleukin-10; MCP-1, monocyte chemoattractant protein-1; MLN, mesenteric lymph node; PA, propionic acid; SFD, standard chow; TNF-α, tumour necrosis factor-alpha.

events (for complete analysis of study results, see Supplementary material online). Oral supplementation of PA led to a significant intra-individual increase of PA concentration in the plasma after 8 weeks (Supplementary material online, *Figure S10A*) but did not affect gut microbiota composition and diversity in a subset of participants for whom faecal samples were available at baseline and at the end of the study (Supplementary material online, *Figure S10B and C*). In line with the finding from the experimental studies, phenotyping of peripheral T cells displayed significant increase of Tregs in the PA group (Supplementary material online, *Figure S11A and B*) without significant alteration of Th17 or Th1 cell numbers (Supplementary material online, *Figure S12A and B*).

Moreover, we evaluated the effect of PA on plasma levels of two distinct factors, fatty acid-binding protein 4 (FABP4) and glucagon, involved in the regulation of glucose metabolism, which were not significantly altered upon oral supplementation with PA (Supplementary material online, *Figure S13*).

Discussion

Despite previous studies implicating atheroprotective effects of the SCFA propionate (PA),[22,33] this is the first study demonstrating the regulatory property of propionate to decrease intestinal cholesterol absorbance via an immunomodulatory pathway. This pathway involves a novel circuit in which increased IL-10 in the intestinal microenvironment down-regulates NPC1l1, the major intestinal cholesterol transporter. Moreover, the clinical relevance of the experimental observations is highlighted for the first time in a randomized, placebo-controlled, double-blind trial evaluating the cholesterol-lowering effect of propionate demonstrating the translational potential of our findings.

Bartolomaeus *et al.*[22] showed vasoprotective effects of PA in a mouse model of angiotensin II-induced hypertensive cardiovascular damage, e.g. by preventing angiotensin II-induced local cardiac proinflammatory immune cell infiltration. Other vasoprotective properties of propionate include blood pressure-lowering effects in mice via endothelial G protein-coupled receptor by dilating resistance vessels in an endothelium-dependent manner.[10] While in these studies lipid-independent models of vascular pathologies were used, our study focused on lipid-modulating properties of PA with subsequent protective effects on atherosclerosis development.

Gut microbial-generated metabolites are important modulators of the host physiologic functions and metabolism.[34] Short-chain fatty acids are derived from anaerobic fermentation of undigested nutrients such as dietary fibre and complex polysaccharides and are

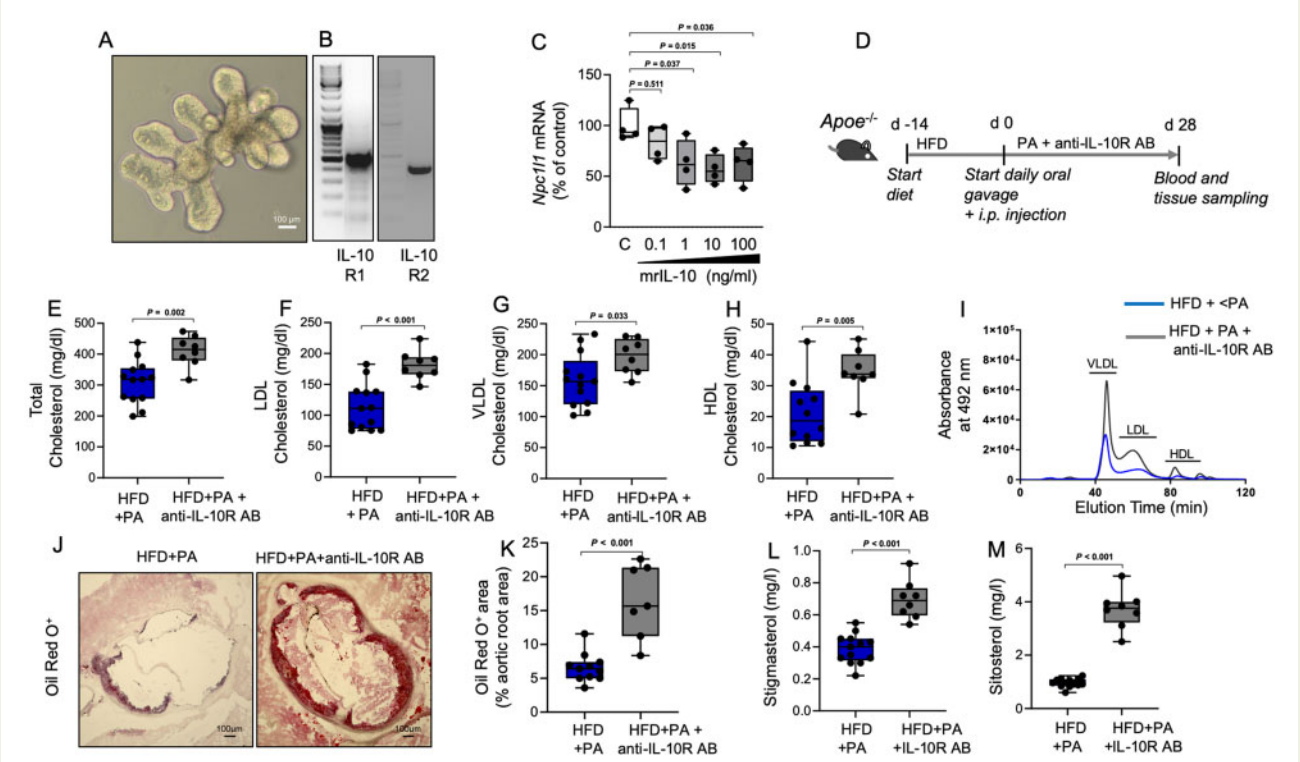

Figure 5 Regulation of Npc1l1 gene expression by interleukin-10 mediates propionate-dependent control of intestinal cholesterol absorption and atheroprotection. (*A*) Representative photomicrograph of a mouse small intestinal epithelial organoid. (*B*) The organoids express both the interleukin-10R1 and interleukin-10R2 receptors, as demonstrated by reverse transcription-polymerase chain reaction. (*C*) Treatment of the organoids with murine recombinant interleukin-10 down-regulated the expression of the *Npc1l1* gene in a dose-dependent manner ($n = 4$ independent biological replicates). (*D*) Interleukin-10 signalling was inhibited by weekly i.p. injection of a monoclonal blocking antibody against the interleukin-10 receptor in high-fat diet-fed *Apoe*$^{-/-}$ mice during the propionic acid treatment period (high-fat diet + propionic acid $n = 13$, high-fat diet + propionic acid + interleukin-10R antibody $n = 8$). (*E–H*) HPLC analysis of blood levels of total cholesterol, low-density lipoprotein cholesterol, very low-density lipoprotein cholesterol and high-density lipoprotein cholesterol in high-fat diet + propionic acid mice in the presence (grey) or absence (blue) of interleukin-10R antibody. (*I*) Representative HPLC-assisted fractionation of plasma lipids. (*J* and *K*) Representative images of Oil Red O-stained aortic root sections (scale bars represent 100 µm) with quantification of lipid deposition (high-fat diet + propionic acid $n = 11$, high-fat diet + propionic acid + interleukin-10R antibody $n = 7$). (*L* and *M*) Analysis of blood levels of the phytosterols stigmasterol and sitosterol at the end of the experiments (high-fat diet + propionic acid $n = 13$, high-fat diet + propionic acid + interleukin-10R antibody $n = 8$). For the analysis in *E–M*, the results for the high-fat diet + propionic acid group were the same results used in *Figure 2*. Data were analysed by a two-tailed unpaired *t*-test. HDL, high-density lipoprotein; HFD, high-fat diet; LDL, low-density lipoprotein; IL-10, interleukin-10; PA, propionic acid; VLDL, very low-density lipoprotein.

considered to have health-promoting properties, e.g. by lowering blood pressure[10,18] and modulating inflammatory responses.[20] Moreover, epidemiological studies have suggested that long-term fibre intake may contribute to preventing dyslipidaemia and atherosclerotic vascular disease,[23] although the underlying mechanisms are only poorly understood.

The current study demonstrates a marked increase in total and LDL cholesterol levels with an increased atherosclerotic lesion size in *Apoe*$^{-/-}$ mice with antibiotic-induced depletion of the gut microbiota as compared to conventionally raised *Apoe*$^{-/-}$ mice. These findings support a functional role of gut microbiota-dependent metabolic pathways in the control of blood cholesterol levels and atherogenesis. In particular, we show here that the SCFA propionate (PA) regulates intestinal expression of the intestinal cholesterol transporter of Niemann-Pick C1-like 1 (NPC1L1) by increasing IL-10 levels in the intestinal microenvironment. Therefore, PA controls circulatory LDL cholesterol levels and attenuates the development of atherosclerosis. The clinical relevance of our experimental findings was demonstrated in a double-blind, placebo-controlled, proof-of-concept trial validating the LDL cholesterol-lowering effect of oral supplementation of propionate in hypercholesterolaemic human subjects. Thus, lowering LDL cholesterol with potential atheroprotective effects by supplementary PA treatment may represent a novel application of a microbiota-derived metabolite. However, further studies are required to evaluate long-term effects of PA on the development of atherosclerosis in humans.

Atherosclerotic cardiovascular diseases are a major global health care burden and a leading cause of mortality and morbidity worldwide.[1] Atherosclerosis starts frequently early in life[35] and further progresses resulting in clinical ACVDs depending on lifetime exposure

Table 1 Baseline characteristics of all randomized study participants

Characteristic	Placebo (*N* = 31)	Propionate (*N* = 31)
Age (years)	51.1 ± 11.6	49.5 ± 12.4
Female sex, *n* (%)	23 (74)	22 (70)
Systolic blood pressure (mmHg)	132.6 ± 18.0	129.1 ± 14.7
Heart rate (beats per minute)	64.2 ± 8.9	59.6 ± 9.6
Body mass index[a]	26.0 ± 3.8	27.3 ± 4.8
Serum creatinine (mg/dL)	0.79 ± 1.3	0.79 ± 1.4
Medical history, *n* (%)		
Hypertension	5 (16.1)	7 (22.5)
Diabetes	0 (0)	1 (3)
Smoker or former smoker	13 (41.9)	19 (61.2)
Cholesterol levels (mg/dL)		
Total	258.4 ± 39.9	254.1 ± 48.8
LDL	185.0 ± 36.1	184.1 ± 46.3
HDL	70.4 ± 19.0	61.1 ± 19.6
Triglyceride (mg/dL)	116.3 ± 43.1	137.6 ± 70.5
Lipoprotein (a) (nmol/L)	58.3 ± 88.0	58.3 ± 103.9

Plus–minus values are means ± SD. There were no significant differences between the two groups. Percentages may not total 100 because of rounding. To convert the values for creatinine to micromoles per litre, multiply by 88.4.
HDL, high-density lipoprotein; LDL, low-density lipoprotein; SD, standard deviation.
[a]The body mass index is the weight in kilograms divided by the square of the height in metres.

to both genetic and environmental causal risk factors.[36] Extensive evidence from epidemiologic, genetic, and clinical intervention studies has shown that LDL is causal in this process.[37] Thus, lowering LDL cholesterol levels is a cornerstone in the prevention of the development and progression of ACVDs.[2]

In addition to traditional cardiovascular risk factors, in recent years, distinct changes in gut microbial composition have been described in the setting of atherosclerotic CVD in a number of case-controlled studies.[34] A large metagenome-wide association study on stools from individuals with atherosclerotic CVD and healthy controls demonstrated an increased abundance of *Enterobacteriaceae* and *Streptococcus* spp. and relatively depleted butyrate and propionate-producing bacteria in patients with atherosclerotic CVD, suggesting a functional role of SCFAs in promoting cardiovascular health.[38] In the vasculature, propionate was demonstrated to mediate vasodilating effects by activating the G protein-coupled receptor 41 in the vascular endothelium and thereby lower blood pressure.[10]

In recent experimental studies, PA was shown to promote the repair capacity after myocardial infarction[39] and protect against hypertensive and ischaemic cardiac injury[22] by maintaining immune homeostasis. Although the underlying mechanisms are not fully understood, intestinal and systemic immune modulation appear to contribute to PA-related cardioprotection. Our observations expand on the recently reported immunomodulatory effects of propionate in the small intestine[20,21] and link the immune-regulatory elements with intestinal lipid control. Our findings reveal a novel regulatory circuit in which PA-induced increases in IL-10, the key Treg cytokine, in the intestinal microenvironment suppress small intestinal NPC1L1 expression, which in turn decreases intestinal cholesterol absorption. Consequently, the resulting decrease in circulatory LDL cholesterol levels attenuates the progression of atherosclerosis in hypercholesterolaemic *Apoe*$^{-/-}$ mice. This hypothesis is further supported by the reversal of the PA-induced effects on cholesterol control and atherosclerosis upon blockade of IL-10 receptor signalling, demonstrating that the underlying mechanism relies on IL-10 signalling in intestinal epithelial cells. Notably, the intestinal immune system, specifically distinct subsets (integrin $\beta7^{+}$) of gut intraepithelial T lymphocytes, has been recently recognized to modulate systemic metabolism, including circulating cholesterol levels.[31] Our findings support the notion that the intestinal immune cell compartment may serve as a novel target to control lipid metabolism.

Our observations align with previous studies showing an increase in Treg number and function by supplementary PA treatment.[21] Mechanistically, it was shown that PA augments the functional capacity of Tregs with increased IL-10 production by enhancing mitochondrial respiration. Moreover, *ex vivo* transcriptome and network connectivity analyses in peripheral blood cells from PA-treated subjects revealed up-regulation of T-cell receptor-associated genes such as CD3ε and CD28 in combination with key cofactors in T-cell activation, such as IL-2 receptor alpha chain, with IL-10 as one of the major gene interaction hubs.[21]

Importantly, a cholesterol-lowering effect has been attributed to IL-10 in clinical studies testing recombinant human IL-10, e.g. in autoimmune and neoplastic diseases.[40,41] However, the underlying pathway of IL-10-mediated regulation of lipid metabolism remains unclear. Our findings reveal a novel regulatory role of IL-10 in intestinal cholesterol absorption by impacting the expression of NPC1L1. Importantly, unlike systemic immunotherapy with recombinant IL-10, local enrichment of IL-10 in the intestinal microenvironment by supplementary PA treatment may prevent adverse side effects while promoting cardiovascular health and atheroprotection.

Notably, PA has been recently reported to stimulate glycogenolysis and hyperglycaemia by increasing plasma concentrations of glucagon and FABP4 through activation of the sympathetic nervous system thereby increasing the risk of insulin resistance.[42] Notably, in our study, PA did affect neither plasma concentrations of glucagon nor FABP4. These results together with unaltered fasting glucose and HbA1C levels under PA treatment suggest that PA treatment with the dosage and duration used in our study does not affect glucose metabolism. The SCFAs PA and butyrate have also been shown in previous studies to activate intestinal gluconeogenesis via a gut-brain neural circuit involving the fatty acid receptor FFAR3.[43] However, this mechanism was suggested to rather promote metabolic benefits in energy homeostasis with reduced adiposity and body weight and better glucose control, including a decrease of hepatic glucose production. Taken together, PA may have diverse effects on glucose control depending on the site of action. Notably, in the current study, many of the study participants from both groups were obese. However, we did not observe any relevant weight alteration in human study participants after 8 weeks PA treatment. This finding may indicate that in humans the cholesterol-lowering property of PA, at least in the short term, is not coupled with weight reduction.

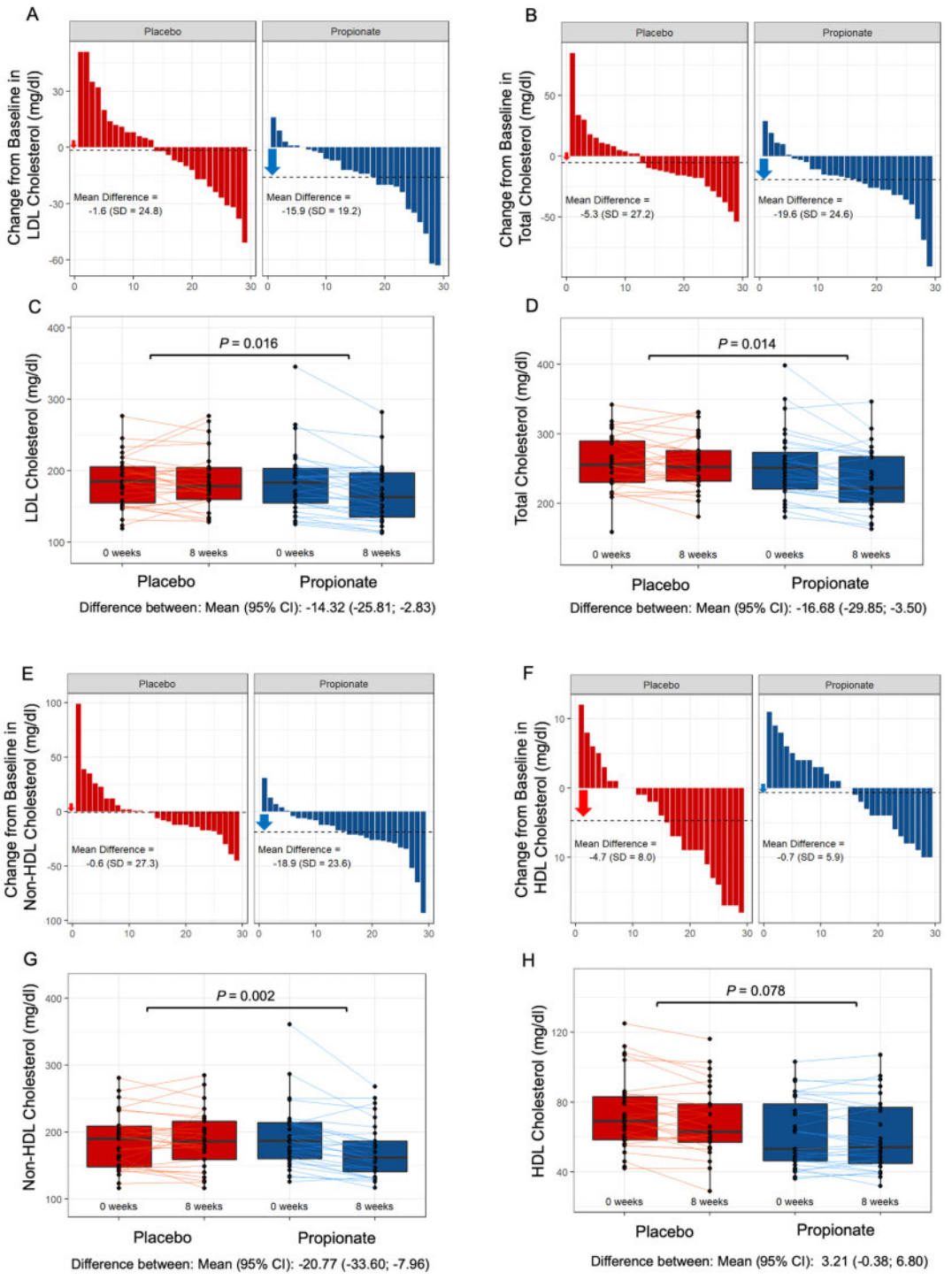

Figure 6 Oral propionate supplementation lowers blood low-density lipoprotein and total cholesterol levels in hypercholesterolaemic humans. (*A* and *B*) Waterfall plots depict the change in low-density lipoprotein and total cholesterol levels a from baseline to Week 8 for each study participant randomly assigned to the placebo group and the propionic acid group. (*C* and *D*) Box plots illustrate the distribution of low-density lipoprotein and total cholesterol levels within the placebo (red) and propionate (blue) groups for each timepoint (baseline and after 8 weeks). (*E* and *F*) Waterfall plots showing the change in non-high-density lipoprotein and high-density lipoprotein cholesterol levels. (*G* and *H*) Box plots demonstrating the distribution of non-high-density lipoprotein and high-density lipoprotein cholesterol levels for each timepoint. The lines depict the raw values at baseline and after 8 weeks. In the box plots, the line in the middle of the box indicates the median, and the lower and upper limits of the box correspond to the 25th and 75th percentiles, respectively. Analysis of covariance was performed to test the delta change between the two groups (placebo $n = 29$, propionate $n = 29$). CI, confidence interval; HDL, high-density lipoprotein; LDL, low-density lipoprotein; SD, standard deviation.

Thus, further long-term studies are warranted to address the long-term metabolic effects of supplementary PA treatment examining glucose, cholesterol, and weight control.

Beyond the atheroprotective role of PA, future studies should evaluate the effects of distinct SCFA on hepatic steatosis and broader analyses of hepatic signalling involved in SCFA-dependent cholesterol metabolism and synthesis should require more attention.

In conclusion, our observations suggest a novel mechanism linking propionate-mediated effects on the gut immune system to intestinal cholesterol regulation, through which exogenous propionate modulates intestinal cholesterol absorption, thereby lowering blood LDL and total cholesterol levels. The clinical relevance of our experimental observations was demonstrated in a proof-of-concept clinical study highlighting the gut immune system as a potential therapeutic target for cardiovascular prevention in humans. Augmentation of intestinal propionate, e.g. by oral supplementation or diet-based strategies, may provide a novel approach to modulate the intestinal immune system and thereby promote cardiovascular health and prevent atherosclerotic CVD. Further studies are needed to evaluate its long-term metabolic effects and consequences on cardiovascular outcome.

Limitations of the study

A potential limitation of the clinical study is the rather short duration of PA treatment of 8 weeks. Thus, it cannot be ruled out that PA-mediated effects may be counteracted by potential negative feedback mechanisms upon long-term application. This needs to be further examined in future studies. Furthermore, the experimental findings were obtained using female mice, and in the clinical trial, the majority is represented by women. However, in a subanalysis of our study cohort, we observed a significant cholesterol-lowering effect also in male study participants upon treatment with PA indicating that the effects are sex-independent. Nevertheless, the sex-independent cholesterol-lowering effects of PA remain to be further confirmed in larger studies.

Although we did not find an alteration in the gut microbial profile upon treatment with PA, it cannot be excluded that the metabolic activity and functional property of distinct bacterial species may be altered in response to oral application of PA and, at least partly, contribute to the lipid-regulatory effects of PA, since distinct bacterial strains, such as Lactobacillus strains, known to metabolize propionate, have also cholesterol-lowering properties.[33]

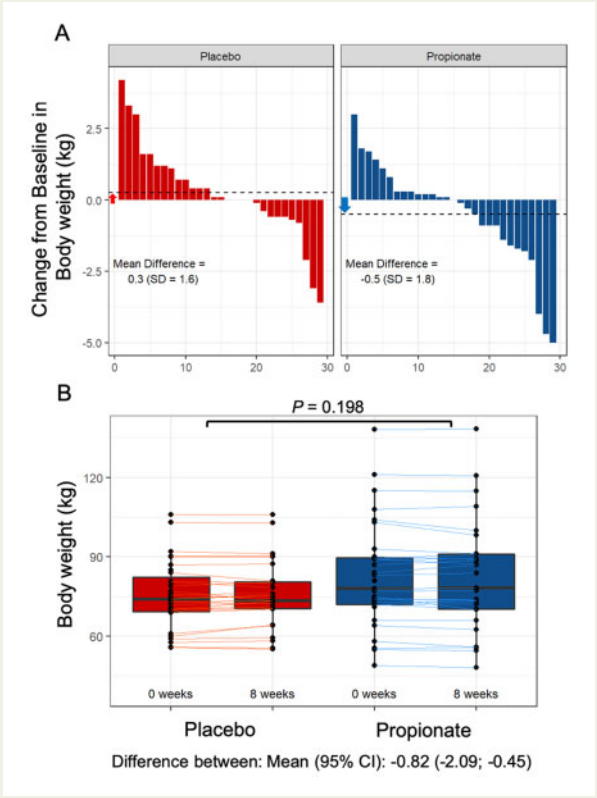

Figure 7 Effect of oral propionate supplementation on body weight. (*A*) Waterfall plots depict the change in body weight from baseline to Week 8 for each study participant randomly assigned to the placebo group and the propionic acid group. (*B*) Box plots illustrate the distribution of body weight within the placebo (red) and propionate (blue) groups for each timepoint (baseline and after 8 weeks). The lines depict the raw values at baseline and after 8 weeks. In the box plots, the line in the middle of the box indicates the median, and the lower and upper limits of the box correspond to the 25th and 75th percentiles, respectively. Analysis of covariance was performed to test the delta change between the two groups (placebo $n = 29$, propionate $n = 29$). CI, confidence interval; SD, standard deviation;

Materials and methods

Mouse experiments

All animals were bred, raised, and housed in the 'Forschungseinrichtungen für Experimentelle Medizin' (FEM, Charité—University Medicine Berlin, Germany) facilities under specific pathogen-free conditions. All experiments were in accordance with the German/European law for animal protection and were approved by the local ethics committee (Das Landesamt für Gesundheit und Soziales Berlin, G0295/16). Animal numbers were calculated with nQuery + nTerim 4.0 software. A two-tailed test with significance levels (α) of 0.05 and a power of 80% was considered with an estimated effect size from our previous work based on the effect of propionate on intestinal Tregs.[20] The mice were maintained on a 12:12-h day: night cycle with constant access to food and water. Adult (16 weeks of age) female C57BL/6J, *Apoe*$^{-/-}$ (Charles River) were age-matched and randomly assigned to either a SCD diet ($n = 12$) (crude fat 4.1%, cholesterol 14 mg/kg; Ssniff, Soest, Germany, E15000) or an HFD ($n = 23$) (crude fat 34.6%, cholesterol 290 mg/kg; Ssniff, Soest, Germany, E1574) for a total of 6 weeks. To study the effect of propionate (PA), calcium propionate (150 mM, Sigma-Aldrich) was administered daily via oral gavage for 4 weeks starting after 2 weeks of HFD (HFD + PA, $n = 13$). Administration of SCFAs by oral gavage has been shown to effectively increase plasma SCFA levels.[44] The mice that were not treated with PA received the vehicle (0.9% sodium chloride) alone ($n = 10$). Inhibition of IL-10 receptor signalling during the period of PA treatment was achieved by intraperitoneal injection of an anti-IL-

Table 2 Adverse events during treatment with placebo or propionate

	Placebo ($n = 31$)	Propionate ($n = 31$)	Total ($n = 62$)
Any adverse event, *n* (%)			
No	20 (64.5)	24 (77.4)	44 (71.0)
Yes	11 (35.5)	7 (22.6)	18 (29.0)
Adverse event, *n* (%)			
Abdominal pain	1 (3.2)	0 (0.0)	1 (1.6)
Abdominal pain and nausea	0 (0.0)	1 (3.2)	1 (1.6)
Acute gastroenteritis	1 (3.2)	0 (0.0)	1 (1.6)
Bipolar disorder	1 (3.2)	0 (0.0)	1 (1.6)
Cold	1 (3.2)	0 (0.0)	1 (1.6)
Diarrhoea	1 (3.2)	0 (0.0)	1 (1.6)
Diarrhoea and cephalgia	0 (0.0)	1 (3.2)	1 (1.6)
Flatulence	1 (3.2)	1 (3.2)	2 (3.2)
Gastroenteritis	1 (3.2)	0 (0.0)	(1.6)
Gastroesophageal reflux	1 (3.2)	1 (3.2)	2 (3.2)
Chest pain and gastroesophageal reflux	1 (3.2)	0 (0.0)	1 (1.6)
Nausea	1 (3.2)	2 (6.5)	3 (4.8)
Nausea and abdominal pain and cephalgia	0 (0.0)	1 (3.2)	(1.6)
Vertigo	1 (3.2)	0 (0.0)	1 (1.6)
Elevation of liver enzymes			
Males: AST => 50, females: AST => 35			
Yes	4 (13.8)	0 (0.0)	4 (6.9)
No	25 (86.2)	29 (100.0)	54 (93.1)
Missing	2 (6.45)	2 (6.45)	4 (6.45)
Males: ALT => 41, females: AST => 31			
Yes	4 (13.8)	5 (17.2)	4 (6.9)
No	25 (86.2)	24 (82.8)	49 (84.5)
Missing	2 (6.4)	2 (6.45)	4 (6.45)

There were no significant differences between the two groups.

10 receptor monoclonal AB (clone 1B1.2, 1 mg per mouse per week, $n = 8$) for 4 weeks starting at the end of Week 2. All mice were sacrificed at the end of Week 6 for the collection of blood and organs. Measured values were excluded in cases of technical failure during the experiment or by statistical testing, as described below. The exact mouse numbers are shown in the respective figures.

Generation of secondary abiotic mice

To generate secondary abiotic mice, quintuple antibiotic treatment (+ABS) was applied for 6 weeks. For this, mice were transferred to sterile cages and treated with a mixture of ampicillin plus sulbactam (1 g/L), vancomycin (500 mg/L), ciprofloxacin (200 mg/L), imipenem (250 mg/L), and metronidazole (1 g/L) in the drinking water. The intestinal colonization status of the mice was controlled once a week by highly sensitive cultural analysis of faecal samples. As early as 3 weeks after the start of broad-spectrum antibiotic treatment, quality controls indicated complete eradication of the intestinal microbiota, validated by negative results from both culture and molecular detection of bacteria using real-time PCR targeting the bacterial 16S rRNA genes. The mice were continuously kept in a sterile environment (autoclaved food and drinking water, sterile filtered antibiotic cocktail) and handled under strict aseptic conditions to avoid contamination.

Lipoprotein separation and metabolite profiling

Plasma samples were subjected to fast-performance liquid chromatography [gel filtration on Superose 6 column (GE Healthcare)]. Different lipoprotein fractions were separated and evaluated based on flow-through time. Cholesterol levels were quantified using an enzymatic assay (Cobas, Roche) according to the manufacturer's protocol. For metabolite profiling, mouse plasma samples (SCD $n = 4$, HFD $n = 4$ and HFD + PA $n = 4$) were analysed using a targeted metabolomics kit (MxP® Quant 500 kit: BIOCRATES Life Sciences AG, Innsbruck, Austria). For analysis of different lipid classes, a combination of liquid chromatography (Agilent 1290 Infinity II LC, Santa Clara, CA, USA) and mass spectrometry (AB SCIEX 5500 QTrap™ mass spectrometer; AB SCIEX, Darmstadt, Germany) was used. After normalization and pre-processing of the data, MetIDQ™ software (Biocrates) was used for peak integration and calculation of metabolite concentrations. Distinct cholesteryl esters were employed for further investigation in this study.

Histology

Following sacrifice, basal segments of the mouse heart were immediately embedded in tissue-freezing medium (Leica) and frozen on dry ice. The tissues were stored at -80°C until further use. Sections of the aortic root (5 µm) were prepared on glass slides (Thermo Scientific, Super frost PLUS) using a Cryostat Microtome (Microm HM 560). Small intestinal tissues were fixed in paraffin. Sections (1–2 µm) were then stained with a polyclonal rabbit AB (Novus Biologicals, # NB400-127) for detection of NPC1L1 protein. Images were analysed and quantified with ImageJ Software.

Quantitative polymerase chain reaction

For quantitative polymerase chain reaction, total RNA from the liver and ileum was isolated with TRIzol reagent (Invitrogen™; 15596026) following the manufacturer's instructions and quantified using absorbance measurements on a NanoDrop (Thermo Scientific™; ND-2000). Enzymatic DNA digestion was performed on total RNA from both tissues using RNase-free DNase I (1 U/µg; Thermo Scientific™; EN0251). Total RNA (1.0 µg) was used for the reverse transcription of hepatic RNA using the High-Capacity cDNA Reverse Transcription Kit (Applied Biosystems™; 4368814), and 0.7 µg of total RNA was used for the reverse transcription of RNA from intestinal tissue using the High-Capacity RNA-to-cDNA Kit (Applied Biosystems™; 4388950).

For intestinal organoids, cDNA synthesis and pre-amplification were performed using the SMART-PCR approach.[45] In brief, 100 ng of total RNA was mixed with 1 mM dNTPs (Thermo Fisher) and 10 µM of oligo-dT primer (5′-AAGCAGTGGTATCAACGCAGAGTACT30VN-3′, where 'N' is any base and 'V' is either 'A', 'C', or 'G'; Biomers), denatured and placed on ice. Then, the first-strand synthesis for each sample was achieved using 5 U/µL Maxima H minus reverse transcriptase (200 U/µL, Invitrogen), 1 U/µL Recombinant RNasin Ribonuclease Inhibitor (PROMEGA), 1× SuperScript VI Reverse Transcriptase (5×, Thermo fisher), 1 M betaine (5 M, Sigma), 10 mM $MgCl^2$+ (1 mM, Thermo fisher), 1 µM ISPCR-TSO (Template Switching Oligos): 5′-AAGCAGTGGTATCAACGCAGAGTACATrGrG+G-3′; two riboguanosines (rG) and one LNA-modified guanosine (+G), and nuclease-free water (Invitrogen). Subsequently, the reverse transcriptase was inactivated, and an adapter-based PCR pre-amplification was carried out using 1× KAPA HiFi HotStart ReadyMix (2×, KAPA ROCHE), 200 nM ISPCR primers (10 µM, 5′AAGCAGTGGTATCAACGCAGAGT-3′, Biomers) and nuclease-free water (Invitrogen). Finally, cDNA was treated with Exonuclease I (NEB) following the manufacturer's instructions.

Relative mRNA expression of hepatic genes (*Cyp7a1, Fxr, Hmgcr, Ldlr, Srebp2, Pcsk9*), intestinal genes (*Abca1, Abcg5, Acat2, Asbt, Npc1l1*, and *Srb1*), and the reference gene *Gapdh* was analysed using TaqMan Gene Expression Assays with the following primers (Applied Biosystems™; 4351372):

Gene	Species	Assay-ID
Abca1	Mouse	Mm00442646_m1
Abcg5	Mouse	Mm00446241_m1
Acat2	Mouse	Mm00782408_s1
Asbt	Mouse	Mm00488258_m1
Cyp7a1	Mouse	Mm00484150_m1
Fxr	Mouse	Mm00436425_m1
Hmgcr	Mouse	Mm01282499_m1
Gapdh	Mouse	Mm99999915_g1
Ldlr	Mouse	Mm01177349_m1
Npc1l1	Mouse	Mm01191973_m1
Pcsk9	Mouse	Mm01263610_m1
Srb1	Mouse	Mm00450234_m1
Srebp2	Mouse	Mm01306292_m1

Relative expression (triple determination) was examined by TaqMan Gene Expression Master Mix (Applied Biosystems™; 4369542) following the manufacturer's instructions.

Reverse transcription-polymerase chain reaction

Reverse transcription-polymerase chain reaction was used to detect the expression of IL10 receptor 1 (IL10R1) in small intestinal organoids. The following gene-specific primer pairs for mouse IL-10R1 and IL-10R2 were manufactured by TIB Molbiol (TIB MOLBIOL Syntheselabor GmbH): IL-10R1: sense 5′ AGG CAG AGG CAG CAG GCC CAG CAG AAT GCT 3′, antisense 5′ TGG AGC CTG GCT AGC TGG TCA CAG TAG GTC 3′; IL-10R2: sense, 5′ GCC AGC TCT AGG AAT GAT TC 3′, antisense 5′ AAT GTT CTT CAA GGT CCA C 3′.[46] The mixture for each reaction was composed of primers (sense and antisense, 10 µM each), BD (Rapidozym; GEN-OPTI-500), $MgCl^2$+ (25 mM; Rapidozym; GEN-OPTI-500), dNTPs (10 µM; Rapidozym; GEN-009-250), and Taq polymerase (5 U/µL; Rapidozym; GEN-OPTI-500) following the manufacturer's instructions. cDNA (2 µL) and RNase-free water were added to reach a volume of 20 µL per well. PCR was performed with an initial denaturation at 95°C for 2 min, followed by 40 cycles of denaturation at 95°C for 30 s, annealing at 64°C for 30 s and extension at 72°C for 1 min. After complete amplification, DNA loading buffer (TaKaRa™; 639285) was added, and the PCR products were visualized by electrophoresis on a 1.5% agarose gel (Agarose; Serva™; 11406.02) (including 20 µL of ethidium bromide and 90 mL of 1× Tris-acetate-EDTA-buffer). PeqGOLD DNA Ladder Mix (VWR Life Science™; 25-2040) served as a molecular weight reference band following the manufacturer's instructions.

Statistical analyses

Database management and statistical analyses were performed with PRISM version 8.2.0 (GraphPad Software Inc., USA), IBM SPSS Statistics 25 (IBM, USA) and R[47] just as additional R packages.[48]

Experimental study

Grubbs' test was performed to identify and exclude outliers. Continuous data were subjected to the Kolmogorov–Smirnov test and Shapiro–Wilk test to determine normality and were expressed as the mean ± standard deviation. A comparison of two groups was

performed by a two-tailed unpaired *t*-test and Mann–Whitney *U* test, as appropriate. To compare >2 groups, one-way ANOVA followed by *post hoc* Tukey's test was performed. Significance was assumed at a two-sided $*P < 0.05$, $**P < 0.01$, or $***P < 0.001$.

Human study

Treatment groups were compared based on analyses of covariance, with difference between measurement at T2 and T0 as the dependent variable, adjusting for measurement at T0. For safety endpoints, we calculated univariate logistic regression models. A two-sided significance level of 5% was applied for all analyses. As we did not correct for multiple testing for secondary endpoints, *P*-values for secondary endpoints have to be interpreted as exploratory analyses. The primary approach to handle missing values was multiple imputation for all endpoints with <40% missing values. As a sensitivity analysis, we also performed a multiple imputation by treatment group for the primary endpoint, and complete-case analyses for all endpoints.

Gut microbiota

The statistical analyses and graphical representations of the microbiota were performed using R v.3.5.1[47] with packages phyloseq v.1.26[49] and ggplot2 v.3. The compositional dissimilarity of the dataset was investigated using the Bray–Curtis dissimilarity metric calculated on proportion-normalized data using the vegdist function from the vegan package. Principal Coordinate Analysis plots were created using the made4 and ggplot2 packages. Permutational MANOVA statistical tests on the Bray–Curtis dissimilarity were performed using the adonis function from the vegan package with 1000 permutations; significance was assumed for *P*-value <0.05. Changes in community diversity were investigated using Shannon Diversity metrics using the estimate_richness function in the phyloseq package.

Supplementary material

Supplementary material is available at *European Heart Journal* online.

Acknowledgements

We thank Manuela Krämer for assistance in profiling the faecal microbiota. The computations microbiota analyses were performed on resources provided by SNIC through Uppsala Multidisciplinary Center for Advanced Computational Science (UPPMAX) under Project SNIC 2018-3-350.

Funding

This study was supported by the Foundation Leducq network 'Gut microbiome as a target for the treatment of cardiometabolic diseases', Sympath ('Systems-medicine of pneumonia-aggravated atherosclerosis', grant number 01ZX1906B) funded by the German Federal Ministry of Education and Research (BMBF), and by grants from the German Heart Research Foundation (DSHF F/28/16), German Center for Cardiovascular Research (DZHK, Rotation Grant), the Else Kröner-Fresenius-Stiftung (2017_A100), and the German Research Foundation (DFG, HA 6951/2-1). A.H. is participant in the BIH-Charité Advanced Clinician Scientist Pilot Program funded by the Charité – Universitätsmedizin Berlin and the Berlin Institute of Health. C.M.S., I.N., and S.L.H. were also supported in part by grants from the National Institutes of Health and the Office of Dietary Supplements (P01HL147823 and R01HL103866). A.N.H. is supported by a Lichtenberg fellowship by Volkswagen Foundation, a Berlin Institute of Health Clinician Scientist grant and German Research Foundation (DFG-TRR241-A05, INST 335/597-1). E.P.C.v.d.V. is supported by a grant from the Interdisciplinary Center for Clinical Research within the faculty of Medicine at the RWTH Aachen University, the DZHK (German Centre for Cardiovascular Research), and the BMBF (German Ministry of Education and Research), the Else Kröner Fresenius-Stiftung (2018_A123), and NWO-ZonMw Veni (91619053). The anti-IL-10R antibody (clone 1B1.2) was kindly provided by the DRFZ core facility.

Conflict of interest: S.L.H. reports being named as co-inventor on pending and issued patents held by the Cleveland Clinic relating to cardiovascular diagnostics and therapeutics, being a paid consultant for P&G, having received research funds from P&G, and Roche Diagnostics, and being eligible to receive royalty payments for inventions or discoveries related to cardiovascular diagnostics or therapeutics from Cleveland HeartLab, Quest Diagnostics, and P&G. All other authors declared no conflict of interest.

Data availability

The data underlying this article will be shared on reasonable request to the corresponding author.

References

1. Townsend N, Wilson L, Bhatnagar P, Wickramasinghe K, Rayner M, Nichols M. Cardiovascular disease in Europe: epidemiological update 2016. *Eur Heart J* 2016;**37**:3232–3245.
2. Mach F, Baigent C, Catapano AL, Koskinas KC, Casula M, Badimon L, Chapman MJ, De Backer GG, Delgado V, Ference BA, Graham IM, Halliday A, Landmesser U, Mihaylova B, Pedersen TR, Riccardi G, Richter DJ, Sabatine MS, Taskinen MR, Tokgozoglu L, Wiklund O; ESC Scientific Document Group. 2019 ESC/EAS Guidelines for the management of dyslipidaemias: lipid modification to reduce cardiovascular risk. *Eur Heart J* 2020;**41**:111–188.
3. Brunner FJ, Waldeyer C, Ojeda F, Salomaa V, Kee F, Sans S, Thorand B, Giampaoli S, Brambilla P, Tunstall-Pedoe H, Moitry M, Iacoviello L, Veronesi G, Grassi G, Mathiesen EB, Söderberg S, Linneberg A, Brenner H, Amouyel P, Ferrières J, Tamosiunas A, Nikitin YP, Drygas W, Melander O, Jöckel KH, Leistner DM, Shaw JE, Panagiotakos DB, Simons LA, Kavousi M, Vasan RS, Dullaart RPF, Wannamethee SG, Risérus U, Shea S, de Lemos JA, Omland T, Kuulasmaa K, Landmesser U, Blankenberg S, Zeller T, Kontto J, Männistö S, Metspalu A, Lackner K, Wild P, Peters A, Meisinger C, Donfrancesco C, Signorini SG, Alver M, Woodward M, Gianfagna F, Costanzo S, Wilsgaard T, Eliasson M, Jørgensen T, Völzke H, Dörr M, Nauck M, Schöttker B, Lorenz T, Makarova N, Twerenbold R, Dallongeville J, Dobson A, Malyutina S, Pajak A, Engström G, Bobak M, Schmidt B, Jääskeläinen T, Niiranen T, Jousilahti P, Giles G, Hodge A, Klotsche J, Magliano DJ, Lyngbakken MN, Hveem K, Pitsavos C, Benjamin EJ, Bakker SJL, Whincup P, Ikram MK, Ingelsson M, Koenig W. Application of non-HDL cholesterol for population-based cardiovascular risk stratification: results from the Multinational Cardiovascular Risk Consortium. *Lancet* 2019;**394**:P2173–P2183.
4. Velagapudi VR, Hezaveh R, Reigstad CS, Gopalacharyulu P, Yetukuri L, Islam S, Felin J, Perkins R, Borén J, Orešič M, Bäckhed F. The gut microbiota modulates host energy and lipid metabolism in mice. *J Lipid Res* 2010;**51**:1101–1112.
5. Wang Z, Roberts AB, Buffa JA, Levison BS, Zhu W, Org E, Gu X, Huang Y, Zamanian-Daryoush M, Culley MK, DiDonato AJ, Fu X, Hazen JE, Krajcik D, DiDonato JA, Lusis AJ, Hazen SL. Non-lethal inhibition of gut microbial trimethylamine production for the treatment of atherosclerosis. *Cell* 2015;**163**:1585–1595.
6. Koeth RA, Wang Z, Levison BS, Buffa JA, Org E, Sheehy BT, Britt EB, Fu X, Wu Y, Li L, Smith JD, Didonato JA, Chen J, Li H, Wu GD, Lewis JD, Warrier M, Brown JM, Krauss RM, Tang WHW, Bushman FD, Lusis AJ, Hazen SL. Intestinal microbiota metabolism of l-carnitine, a nutrient in red meat, promotes atherosclerosis. *Nat Med* 2013;**19**:576–585.
7. Jonsson AL, Caesar R, Akrami R, Reinhardt C, Hållenius FF, Borén J, Bäckhed F. Impact of gut microbiota and diet on the development of atherosclerosis in ApoE-/- mice, Arterioscler. *Thromb Vasc Biol* 2018;**38**:2318–2326.
8. Kasahara K, Krautkramer KA, Org E, Romano KA, Kerby RL, Vivas EI, Mehrabian M, Denu JM, Bäckhed F, Lusis AJ, Rey FE. Interactions between Roseburia

intestinalis and diet modulate atherogenesis in a murine model. *Nat Microbiol* 2018;**3**:1461–1471.
9. Brandsma E, Kloosterhuis NJ, Koster M, Dekker DC, Gijbels MJJ, Van Der Velden S, Ríos-Morales M, Van Faassen MJR, Loreti MG, De Bruin A, Fu J, Kuipers F, Bakker BM, Westerterp M, De Winther MPJ, Hofker MH, Van De Sluis B, Koonen DPY. A proinflammatory gut microbiota increases systemic inflammation and accelerates atherosclerosis. *Circ Res* 2019;**124**:94–100.
10. Natarajan N, Hori D, Flavahan S, Steppan J, Flavahan NA, Berkowitz DE, Pluznick JL. Microbial short chain fatty acid metabolites lower blood pressure via endothelial G protein-coupled receptor 41. *Physiol Genomics* 2016;**48**:826–834.
11. Nemet I, Saha PP, Gupta N, Zhu W, Romano KA, Skye SM, Cajka T, Mohan ML, Li L, Wu Y, Funabashi M, Ramer-Tait AE, Naga Prasad SV, Fiehn O, Rey FE, Tang WHW, Fischbach MA, DiDonato JA, Hazen SL. A cardiovascular disease-linked gut microbial metabolite acts via adrenergic receptors. *Cell* 2020;**180**:862–877.e22.
12. Wang Z, Klipfell E, Bennett BJ, Koeth R, Levison BS, DuGar B, Feldstein AE, Britt EB, Fu X, Chung Y-M, Wu Y, Schauer P, Smith JD, Allayee H, Tang WHW, DiDonato JA, Lusis AJ, Hazen SL. Gut flora metabolism of phosphatidylcholine promotes cardiovascular disease. *Nature* 2011;**472**:57–63.
13. Tang WHW, Wang Z, Levison BS, Koeth RA, Britt EB, Fu X, Wu Y, Hazen SL. Intestinal microbial metabolism of phosphatidylcholine and cardiovascular risk. *N Engl J Med* 2013;**368**:1575–1584.
14. Tang WHW, Wang Z, Kennedy DJ, Wu Y, Buffa JA, Agatisa-Boyle B, Li XS, Levison BS, Hazen SL. Gut microbiota-dependent trimethylamine N-oxide (TMAO) pathway contributes to both development of renal insufficiency and mortality risk in chronic kidney disease. *Circ Res* 2014;**116**:448–455.
15. Haghikia A, Li XS, Liman TG, Bledau N, Schmidt D, Zimmermann F, Kränkel N, Widera C, Sonnenschein K, Haghikia A, Weissenborn K, Fraccarollo D, Heimesaat MM, Bauersachs J, Wang Z, Zhu W, Bavendiek U, Hazen SL, Endres M, Landmesser U. Gut microbiota-dependent trimethylamine N-oxide predicts risk of cardiovascular events in patients with stroke and is related to proinflammatory monocytes. *Arterioscler Thromb Vasc Biol* 2018;**38**:2225–2235.
16. Schiattarella GG, Sannino A, Toscano E, Giugliano G, Gargiulo G, Franzone A, Trimarco B, Esposito G, Perrino C. Gut microbe-generated metabolite trimethylamine-N-oxide as cardiovascular risk biomarker: a systematic review and dose-response meta-analysis. *Eur Heart J* 2017;**38**:2948–2956.
17. Koh A, De Vadder F, Kovatcheva-Datchary P, Bäckhed F. From dietary fiber to host physiology: short-chain fatty acids as key bacterial metabolites. *Cell* 2016;**165**:1332–1345.
18. Kaye DM, Shihata W, Jama HA, Tsyganov K, Ziemann M, Kiriazis H, Horlock D, Vijay A, Giam B, Vinh A, Johnson C, Fiedler A, Donner D, Snelson M, Coughlan MT, Phillips S, Du X-J, El-Osta A, Drummond G, Lambert GW, Spector T, Valdes AM, Mackay CR, Marques FZ. Deficiency of prebiotic fibre and insufficient signalling through gut metabolite sensing receptors leads to cardiovascular disease. *Circulation* 2020;**141**:1393–1403.
19. Smith PM, Howitt MR, Panikov N, Michaud M, Gallini CA, Bohlooly-Y M, Glickman JN, Garrett WS. The microbial metabolites, short-chain fatty acids, regulate colonic Treg cell homeostasis. *Science* 2013;**341**:569–573.
20. Haghikia A, Jörg S, Duscha A, Berg J, Manzel A, Waschbisch A, Hammer A, Lee DH, May C, Wilck N, Balogh A, Ostermann AI, Schebb NH, Akkad DA, Grohme DA, Kleinewietfeld M, Kempa S, Thöne J, Demir S, Müller DN, Gold R, Linker RA. Dietary fatty acids directly impact central nervous system autoimmunity via the small intestine. *Immunity* 2015;**43**:817–829.
21. Duscha A, Gisevius B, Hirschberg S, Yissachar N, Stangl GI, Eilers E, Bader V, Haase S, Kaisler J, David C, Schneider R, Troisi R, Zent D, Hegelmaier T, Dokalis N, Gerstein S, Del Mare-Roumani S, Amidror S, Staszewski O, Poschmann G, Stühler K, Hirche F, Balogh A, Kempa S, Träger P, Zaiss MM, Holm JB, Massa MG, Nielsen HB, Faissner A, Lukas C, Gatermann SG, Scholz M, Przuntek H, Prinz M, Forslund SK, Winklhofer KF, Müller DN, Linker RA, Gold R, Haghikia A. Propionic acid shapes the multiple sclerosis disease course by an immunomodulatory mechanism. *Cell* 2020;**180**:1067–1080.e16.
22. Bartolomaeus H, Balogh A, Yakoub M, Homann S, Markó L, Höges S, Tsvetkov D, Krannich A, Wundersitz S, Avery EG, Haase N, Kräker K, Hering L, Maase M, Kusche-Vihrog K, Grandoch M, Fielitz J, Kempa S, Gollasch M, Zhumadilov Z, Kozhakhmetov S, Kushugulova A, Eckardt KU, Dechend R, Rump LC, Forslund SK, Müller DN, Stegbauer J, Wilck N. Short-chain fatty acid propionate protects from hypertensive cardiovascular damage. *Circulation* 2019;**139**:1407–1421.
23. Crowe FL, Key TJ, Appleby PN, Overvad K, Schmidt EB, Egeberg R, Tjønneland A, Kaaks R, Teucher B, Boeing H, Weikert C, Trichopoulou A, Ouranos V, Valanou E, Masala G, Sieri S, Panico S, Tumino R, Matullo G, Bueno-De-Mesquita HB, Boer JMA, Beulens JWJ, Van Der Schouw YT, Quirós JR, Buckland G, Sánchez MJ, Dorronsoro M, Huerta JM, Moreno-Iribas C, Hedblad B, Jansson JH, Wennberg P, Khaw KT, Wareham N, Ferrari P, Illner AK, Chuang SC, Norat T, Danesh J, Riboli E. Dietary fibre intake and ischaemic heart disease mortality: the European Prospective Investigation into Cancer and Nutrition-Heart study. *Eur J Clin Nutr* 2012;**66**:950–956.
24. Klingenberg R, Gerdes N, Badeau RM, Gisterå A, Strodthoff D, Ketelhuth DFJ, Lundberg AM, Rudling M, Nilsson SK, Olivecrona G, Zoller S, Lohmann C, Lüscher TF, Jauhiainen M, Sparwasser T, Hansson GK. Depletion of FOXP3+ regulatory T cells promotes hypercholesterolemia and atherosclerosis. *J Clin Invest* 2013;**123**:1323–1334.
25. Michos ED, McEvoy JW, Blumenthal RS. Lipid management for the prevention of atherosclerotic cardiovascular disease. *N Engl J Med* 2019;**381**:1557–1567.
26. Altmann SW, Davis HR, Zhu LJ, Yao X, Hoos LM, Tetzloff G, Iyer SPN, Maguire M, Golovko A, Zeng M, Wang L, Murgolo N, Graziano MP. Niemann-pick C1 like 1 protein is critical for intestinal cholesterol absorption. *Science* 2004;**303**:1201–1204.
27. Dawson PA, Haywood J, Craddock AL, Wilson M, Tietjen M, Kluckman K, Maeda N, Parks JS. Targeted deletion of the ileal bile acid transporter eliminates enterohepatic cycling of bile acids in mice. *J Biol Chem* 2003;**278**:33920–33927.
28. Silbernagel G, Fauler G, Genser B, Drechsler C, Krane V, Scharnagl H, Grammer TB, Baumgartner I, Ritz E, Wanner C, März W. Intestinal cholesterol absorption, treatment with atorvastatin, and cardiovascular risk in hemodialysis patients. *J Am Coll Cardiol* 2015;**65**:2291–2298.
29. Huch M, Koo BK. Modeling mouse and human development using organoid cultures. *Development* 2015;**142**:3113–3125.
30. Arpaia N, Campbell C, Fan X, Dikiy S, Van Der Veeken J, Deroos P, Liu H, Cross JR, Pfeffer K, Coffer PJ, Rudensky AY. Metabolites produced by commensal bacteria promote peripheral regulatory T-cell generation. *Nature* 2013;**504**:451–455.
31. He S, Kahles F, Rattik S, Nairz M, McAlpine CS, Anzai A, Selgrade D, Fenn AM, Chan CT, Mindur JE, Valet C, Poller WC, Halle L, Rotllan N, Iwamoto Y, Wojtkiewicz GR, Weissleder R, Libby P, Fernández-Hernando C, Drucker DJ, Nahrendorf M, Swirski FK. Gut intraepithelial T cells calibrate metabolism and accelerate cardiovascular disease. *Nature* 2019;**566**:115–119.
32. Biton M, Haber AL, Rogel N, Burgin G, Beyaz S, Schnell A, Ashenberg O, Su CW, Smillie C, Shekhar K, Chen Z, Wu C, Ordovas-Montanes J, Alvarez D, Herbst RH, Zhang M, Tirosh I, Dionne D, Nguyen LT, Xifaras ME, Shalek AK, von Andrian UH, Graham DB, Rozenblatt-Rosen O, Shi HN, Kuchroo V, Yilmaz OH, Regev A, Xavier RJ. T helper cell cytokines modulate intestinal stem cell renewal and differentiation. *Cell* 2018;**175**:1307–1320.e22.
33. Wang J, Zhang H, Chen X, Chen Y, Menghebilige, Bao Q. Selection of potential probiotic lactobacilli for cholesterol-lowering properties and their effect on cholesterol metabolism in rats fed a high-lipid diet. *J Dairy Sci* 2012;**95**:1645–1654.
34. Tang WHW, Bäckhed F, Landmesser U, Hazen SL. Intestinal microbiota in cardiovascular health and disease: JACC state-of-the-art review. *J Am Coll Cardiol* 2019;**73**:2089–2105.
35. Berenson GS, Srinivasan SR, Bao W, Newman WP, Tracy RE, Wattigney WA. Association between multiple cardiovascular risk factors and atherosclerosis in children and young adults. *N Engl J Med* 1998;**338**:1650–1656.
36. Ray KK, Laufs U, Cosentino F, Lobo MD, Landmesser U. The year in cardiology: cardiovascular prevention. *Eur Heart J* 2020;**41**:1157–1163.
37. Ference BA, Ginsberg HN, Graham I, Ray KK, Packard CJ, Bruckert E, Hegele RA, Krauss RM, Raal FJ, Schunkert H, Watts GF, Borén J, Fazio S, Horton JD, Masana L, Nicholls SJ, Nordestgaard BG, van de Sluis B, Taskinen M-R, Tokgözoglu L, Landmesser U, Laufs U, Wiklund O, Stock JK, Chapman MJ, Catapano AL. Low-density lipoproteins cause atherosclerotic cardiovascular disease. 1. Evidence from genetic, epidemiologic, and clinical studies. A consensus statement from the European Atherosclerosis Society Consensus Panel. *Eur Heart J* 2017;**38**:2459–2472.
38. Jie Z, Xia H, Zhong SL, Feng Q, Li S, Liang S, Zhong H, Liu Z, Gao Y, Zhao H, Zhang D, Su Z, Fang Z, Lan Z, Li J, Xiao L, Li J, Li R, Li X, Li F, Ren H, Huang Y, Peng Y, Li G, Wen B, Dong B, Chen JY, Geng QS, Zhang ZW, Yang H, Wang J, Wang J, Zhang X, Madsen L, Brix S, Ning G, Xu X, Liu X, Hou Y, Jia H, He K, Kristiansen K. The gut microbiome in atherosclerotic cardiovascular disease. *Nat Commun* 2017;**8**:845.
39. Tang TWH, Chen HC, Chen CY, Yen CYT, Lin CJ, Prajnamitra RP, Chen LL, Ruan SC, Lin JH, Lin PJ, Lu HH, Kuo CW, Chang CM, Hall AD, Vivas EI, Shui JW, Chen P, Hacker TA, Rey FE, Kamp TJ, Hsieh PCH. Loss of gut microbiota alters immune system composition and cripples postinfarction cardiac repair. *Circulation* 2019;**139**:647–659.
40. Kimball AB, Kawamura T, Tejura K, Boss C, Hancox AR, Vogel JC, Steinberg SM, Turner ML, Blauvelt A. Clinical and immunologic assessment of patients with psoriasis in a randomized, double-blind, placebo-controlled trial using recombinant human interleukin 10. *Arch Dermatol* 2002;**138**:1341–1346.
41. Chan IH, Van Hoof D, Abramova M, Bilardello M, Mar E, Jorgensen B, McCauley S, Bal H, Oft M, Van Vlasselaer P, Mumm JB. Pegylated il-10 activates kupffer cells to control hypercholesterolemia. *PLoS One* 2016;**11**:e0156229.
42. Tirosh A, Calay ES, Tuncman G, Claiborn KC, Inouye KE, Eguchi K, Alcala M, Rathaus M, Hollander KS, Ron I, Livne R, Heianza Y, Qi L, Shai I, Garg R, Hotamisligil GS. The short-chain fatty acid propionate increases glucagon and

FABP4 production, impairing insulin action in mice and humans. *Sci Transl Med* 2019;**11**:eaav0120.
43. Vadder FD, Kovatcheva-Datchary P, Goncalves D, Vinera J, Zitoun C, Duchampt A, Bäckhed F, Mithieux G. Microbiota-generated metabolites promote metabolic benefits via gut-brain neural circuits. *Cell* 2014;**156**:84–96.
44. Shubitowski TB, Poll BG, Natarajan N, Pluznick JL. Short-chain fatty acid delivery: assessing exogenous administration of the microbiome metabolite acetate in mice. *Physiol Rep* 2019;**7**:e14005.
45. Picelli S, Björklund ÅK, Faridani OR, Sagasser S, Winberg G, Sandberg R. Smart-seq2 for sensitive full-length transcriptome profiling in single cells. *Nat Methods* 2013;**10**:1096–1098.
46. Denning TL, Campbell NA, Song F, Garofalo RP, Klimpel GR, Reyes VE, Ernst PB. Expression of IL-10 receptors on epithelial cells from the murine small and large intestine. *Int Immunol* 2000;**12**:133–139.
47. R Core Team. *R: A Language and Environment for Statistical Computing*. Vienna, Austria: R Foundation for Statistical Computing; 2018.
48. Wickham H, Averick M, Bryan J, Chang W, McGowan L, François R, Grolemund G, Hayes A, Henry L, Hester J, Kuhn M, Pedersen T, Miller E, Bache S, Müller K, Ooms J, Robinson D, Seidel D, Spinu V, Takahashi K, Vaughan D, Wilke C, Woo K, Yutani H. Welcome to the tidyverse. *J Open Source Softw* 2019;**4**:1686.
49. McMurdie PJ, Holmes S. Phyloseq: an R package for reproducible interactive analysis and graphics of microbiome census data. *PLoS One* 2013;**8**:e61217.